Electronic band structures of monolayer hexagonal boron nitride on TaC(111)

M.Terai, Y.Gamo, N.Hasegawa, and C.Oshima

Department of Applied Physics, Waseda University, 3-4-1 Okubo, Sinjuku-ku, Tokyo 169, Japan

(Received: Jan. 30, 1997 Accepted: Man. 7, 1997)

Abstract

By using angle-resolved ultraviolet photoelectron spectroscopy and X-ray photoelectron spectroscopy, we have investigated the electronic properties of monolayer film of hexagonal boron nitride (*h*-BN) formed on TaC(111). The observed valence-bands have agreed with those of monolayer *h*-BN on Pd and Pt(111), which are also very close to the calculated σ and π bands of bulk *h*-BN. The observed π band is much different from the π band of *h*-BN on Ni(111). Differing from the case of the monolayer graphite which interacts strongly with TaC(111), the interfacial bonding between monolayer *h*-BN and the same substrate is weak likely to physisorption.

1. Introduction

Hexagonal boron nitride (*h*-BN) is a highly anisotropic insulator isostructural to semimetallic graphite. In previous works [1-2], the band structures of monolayer *h*-BN formed on Ni, Pd, and Pt(111) surfaces were reported; while the band structures of monolayer *h*-BN on Pd(111) agreed with those on Pt(111) perfectly, only the π band of the monolayer *h*-BN on Ni(111) shifts about 1 eV deeper from those of the other two cases, which means that the overlayer is bonded more strongly onto Ni(111) than the others. In the monolayer graphite (MG) formed on the (111) surfaces of Ni and transition metal carbide (TMCs) such as TaC and TiC, the band structures were largely modified from the bulk ones by the interfacial interaction; namely these MG are bonded chemically onto these chemically reactive surfaces[3-6].

In this study, we have investigated electronic band structures of monolayer *h*-BN formed on TaC(111) surface, one of the chemically reactive surfaces, by using X-ray photoelectron spectroscopy (XPS) and angle-resolved ultraviolet photoelectron spectroscopy (ARUPS). Comparison of the observed valence-band structures of monolayer *h*-BN/TaC(111) with the previous works indicates that the interfacial bonding is weak likely to the physisorption.

2. Experimental

The experiments were done in a ultrahigh vacuum (UHV) chamber with a base pressure of ~1×10^{-8} Pa. The vacuum chamber was equipped with a low energy electron-diffraction (LEED) optics, a hemispherical energy analyzer, an ultraviolet discharge lamp, an X-ray source, and a gas introduction system. We used unpolarized HeI ($h\nu$=21.2 eV) and HeII ($h\nu$=40.8 eV) resonance lines as the primary UV lights for ARUPS, and characteristic X-rays of Mg Kα (1253.6 eV) for XPS. The energy resolution of the electron energy analyzer for the UPS and XPS measurements was set to be 0.2 and 0.5 eV, respectively. Because of the linewidth of the X-rays of Mg kα (0.7 eV) , the overall resolution was about 0.9 eV for XPS, 0.2 eV for UPS. In this experiment, we have prepared a clean TaC(111) substrate in the normal way. One face of the specimen was mechanically polished to a mirror finish, and was cleaned finally by flash heatings up to 1500°C in UHV below 3×10^{-7} Pa. After several heatings, the LEED pattern of the clean surface showed sharp diffraction spots, corresponding to a 1×1 atomic structure in a low background. No impurities such as oxygen or contaminated carbon were found in XPS spectra. We have formed monolayer *h*-BN on this clean surface by chemical vapor deposition.

3. Results and Discussion

The monolayer *h*-BN film was grown epitaxially on clean TaC(111) at 800°C by decomposition of borazine ($B_3N_3H_6$) gas. Figure 1 shows the XPS spectra in the N1s and B1s energy regions obtained during the growing process. The XPS peak of $Ta2p_{3/2}$ is located at the binding energy of ~407 eV. After the

exposure of 200L, B1s and N1s peaks appeared at the binding energies of 195.1 eV and 402.7 eV, respectively. Because of the large reduction of surface reactivity due to the *h*-BN film formation, the growth rate of the *h*-BN becomes extremely low by the overlayer formation [2]. No change was observed in the intensities of the B 1s and N 1s XPS peak after the exposures above 200L, and hence, the growth of monolayer *h*-BN was completed at the exposure less than 200L.

Figure 2(a) and (b) shows an observed LEED pattern of monolayer *h*-BN/TaC(111) and its schematic picture, respectively. The observed pattern showed an incommensurate relation between the monolayer *h*-BN and the substrate. Open circles in Fig. 2(b) indicate diffraction spots due to the overlayer, double circles due to substrate. Any other spots shown by small dots come from the multiple diffraction; they are located at the positions where the wave vector parallel to the surface $q_{//}$ satisfies the following formula:

$$q_{//} = (l_1 h_1 + l_2 h_2) + (m_1 s_1 + m_2 s_2) \qquad (1)$$

Here, l_1, l_2, m_1, and m_2 are integers. Vectors, s_1 and s_2 denote the reciprocal-lattice unit vectors of the substrate, and vectors, h_1 and h_2 denote those of the overlayer. The observed LEED pattern indicates that the monolayer *h*-BN overlayer has a single-domain structure on the TaC(111) surface, of which azimuthal-epitaxial relation was as follows; *h*-BN <11$\bar{2}$0> // TaC <1$\bar{1}$0>. The in-plane lattice constant of the monolayer *h*-BN is 2.53Å±0.02Å, which is good agreement with the bulk one, 2.50Å.

Figure 3(a) and (b) shows typical ARUPS spectra of the monolayer *h*-BN/TaC(111) excited along the $\overline{\Gamma K}$ direction of the surface Brillouin zone (SBZ) by HeI and HeII resonance lines. The emission angle referred to the surface normal is denoted for each

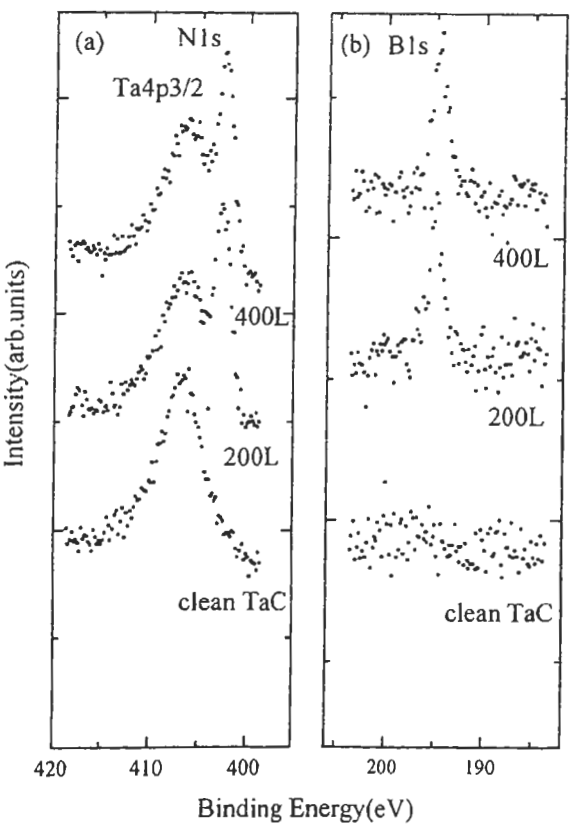

Fig.1 XPS spectra in the energy regions of (a) N 1s and (b) B 1s levels of clean TaC(111), and *h*-BN covered surfaces prepared by 200L and 400L exposure of borazine.

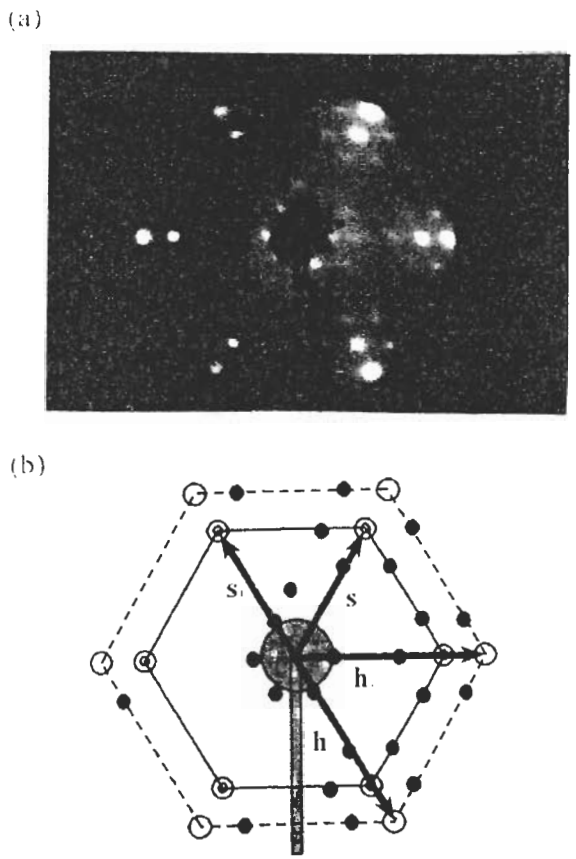

Fig.2 (a) A typical LEED pattern of the monolayer *h*-BN/TaC(111) and (b) its schematic picture. The primary energy was 64 eV. Vectors, s_1 and s_2 denote the reciprocal-lattice unit vectors of the substrate, respectively, and h_1 and h_2 are reciprocal unit vectors of the overlayer. Small dots represent satellite spots due to the multiple diffraction.

spectrum. In both Fig. 3(a) and 3(b), we observed almost dispersionless peaks located at ~5eV and just below the Fermi level (E_F). Since these peaks have been also observed for the clean TaC(111) surface, they are attributed to the emission from either the Ta 5d - C 2p bulk bands or the surface induced bands mainly composed of Ta 5d orbitals[7].

In Fig. 3(a), there are two series of peaks due to the σ bands of the monolayer *h*-BN which are indicated by dotted lines. These peaks shift downwards as emission angle increases. In Fig. 3(b), the peaks due to the π band of monolayer h-BN are observed around the normal emission and the peaks due to the σ band are also observed at high emission angles. In Fig. 4, we have mapped the valence-bands in the SBZ of monolayer *h*-BN using the conservation laws of parallel component of wave vector and energy. The detected wave vector ($k_{//}$ of the initial state) is described from the conservation low in the following way.

$$k_{//} = \left[2m\left(h\nu - \phi - E_B^F\right)\right]^{1/2} \sin\theta \qquad (2)$$

where is the rest mass of electron, hν, the photon energy for excitation, ϕ, the work function of the monolayer *h*-BN/TaC(111) (4.2eV, determined in the previous work), θ, the emission angle from the surface normal, and, E_B^F binding energy. We have carefully excluded the substrate peaks from the comparison with the clean TaC(111) spectra. In Fig. 4, we plotted the experimental valence-band structures of the monolayer *h*-BN on Ni, Pd, and Pt(111) surfaces[1] for comparison. Open marks represent the data points obtained with HeI resonance line, solid marks with HeII resonance line. It should be noted that the binding energies of all the peaks are plotted from the vacuum level (E_V), not from the Fermi level (E_F).

The σ band structures observed for the four substrates agreed well with each other. The same tendency was also found in the binding energies of the core levels. In table I, we tabulate the binding energies of both the N 1s

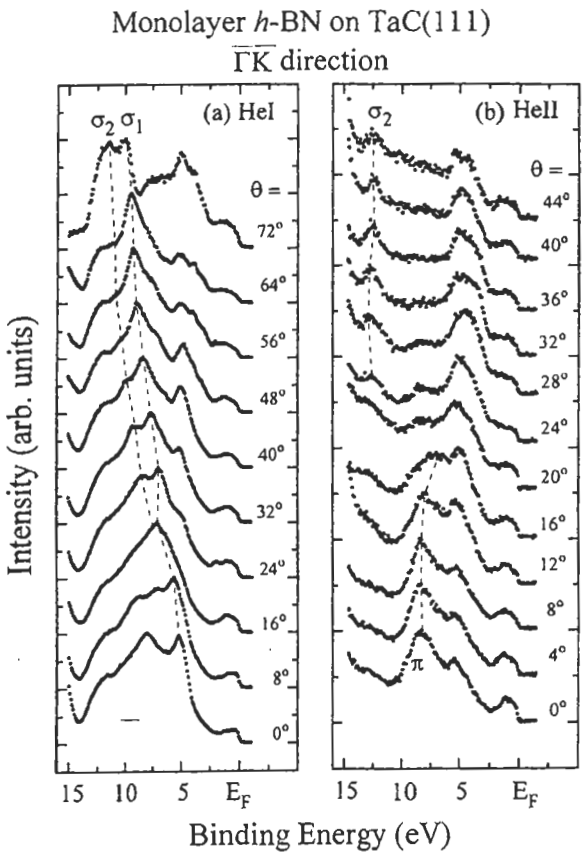

Fig.3 Typical ARUPS spectra of the monolayer *h*-BN/TaC(111) excited by (a) HeI ($h\nu$=21.2 eV) and (b) HeII ($h\nu$=40.8 eV) resonance lines. The emission angle from the surface normal is denoted for each spectrum.

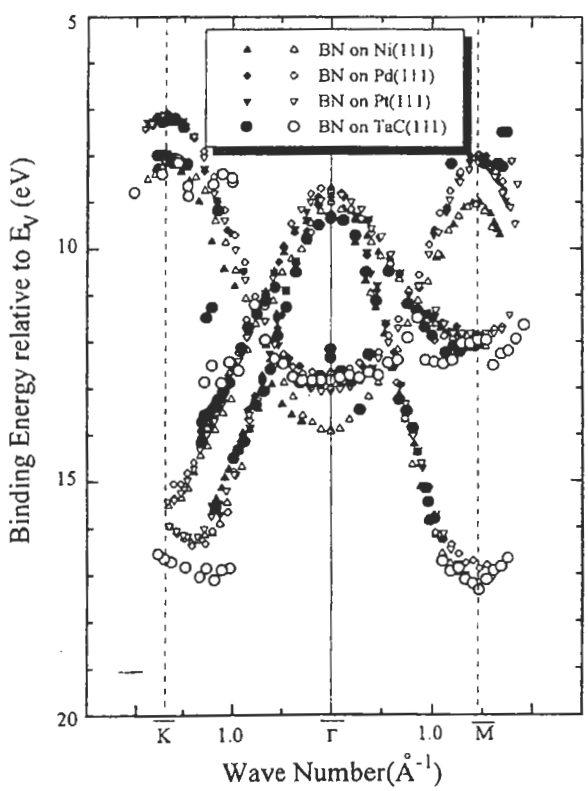

Fig.4 Experimental valence-band structures of the monolayer *h*-BN formed on Ni(111), Pd(111), Pt(111) [1], and TaC(111). Open marks denote the data points obtained with HeI resonance line and solid marks with HeII resonance line.

Table I Experimental values (in eV) for the work funcion of the clean-and BN-covered surfacs, the binding energies of the N 1S and B 1s XPS peaks, and those of the π and σ bands at the $\bar{\Gamma}$ point. E_B^F is referred to the Fermi level and E_B^V to the vacuum level.

	Work Function		N 1s		B 1s		π band(at $\bar{\Gamma}$)		σ band(at $\bar{\Gamma}$)	
Substrate	Clean	BN-covered	E_B^F	E_B^V	E_B^F	E_B^V	E_B^F	E_B^V	E_B^F	E_B^V
Ni(111)	5.3	3.6	399.1	402.7	191.3	194.9	10.3	13.9	5.3	8.9
Pd(111)	5.3	4.0	398.2	402.2	190.5	194.5	8.7	12.7	4.8	8.8
Pt(111)	5.8	4.9	397.3	402.2	189.7	194.6	8.2	13.1	3.9	8.8
TaC(111)	4.7	4.2	398.5	402.7	190.9	195.1	8.5	12.7	5.1	9.3

and B 1s peaks, and π and σ bands at the $\bar{\Gamma}$ point. The experimental work function of the clean and monolayer *h*-BN covered surfaces are also cited. It is clearly seen Table I that the binding energies referred to $E_F(E_B^F)$ vary from one substrate to the other, while those referred to $E_V(E_B^V)$ are almost the same. Since the work function of the substrates has changed upon the formation of the monolayer *h*-BN, the monolayer *h*-BN sits outside the surface barrier which determines the work function and the energies of the overlayer are aligned to E_V. This nature of the bond between the monolayer *h*-BN and the metal surface resembles that of the rare-gas which physisorbs on several metals [8-13]. This facts have already been pointed out for *h*-BN on Pd and Pt in the previous paper[1]. In addition, the π band structure observed for the *h*-BN/TaC(111) agrees quite well with those of the Pd and Pt(111), but differs from the case of Ni(111); the π band locates at the deeper binding energy by ~1eV on Ni(111) than the other substrates. All the experimental results show the physisorption of monolayer h-BN on TaC(111), which is in clear contrast to the MG on the same surface. The MG overlayer interacts strongly not only with Ni(111), but also with TMC(111) surfaces by mixing of the π states with the d states of the substrates.

What is the origin of the difference in the interfacial bonding between these h-BN and MG overlayers? The topmost layer of the clean TaC(111) consists of Ta metal atoms[7], of which the d electrons construct the surface-resonance electronic states near E_F. They are located in the shallow regions from E_F to 2eV[7,14]. On the other hand, the *h*-BN has the wide gap of ~4.5eV and the MG is the typical semi-metal with zero gap. The absence of the π states in *h*-BN around E_F is presumably the origin for no orbital mixing.

Lastly, we would like to comment the exception case of bonding character of *h*-BN on Ni(111). The in-plane lattice constant of h-BN (2.50Å) is very close to the surface lattice constant of Ni(111), 2.49Å (in comparison, 3.15Å for TaC(111), 2.75Å for Pd(111), 2.77Å for Pt(111)) and the commensurate h-BN films grew on Ni(111). Recent LEED intensity analysis indicated the narrow interlayer spacing between monolayer *h*-BN and topmost layer of Ni atoms, ~2.1Å[15]. The Ab-intio calculation for this atomic structure indicates the clear orbital mixing of π bands with sp electrons of Ni atoms[16]. Therefore, the surface electronic states of the substrates and the lattice matching are important factors to generate the orbital mixing.

4. Conclusion

The electronic structures of monolayer *h*-BN/TaC(111) have been measured by XPS and ARUPS. Differing from MG, the interfacial bonding between monolayer *h*-BN and TaC(111) is weak likely to physisorption.

References

1. A.Nagashima, N.Tejima, Y.Gamo and C.Oshima, Phys.Rev.Lett.75, 3918(1995)
2. A.Nagashima, N.Tejima, Y.Gamo, T.Kawai and C.Oshima, Phys.Rev.B 51,4606(1995)
3. A.Nagashima, K.Nuka, K.Satoh, H.Itoh, T.Ichinokawa, S.Otani and C.Oshima, Surf.Sci.,287/288,609(1993)
4. A.Nagashima, K.Nuka, H.Itoh, T.Ichinokawa, S.Otani and C.Oshima, Surf.Sci,291,93(1993)
5. A.Nagashima, H.Itoh, T.Ichinokawa, S.Otani and C.Oshima, Phys.Rev.B 50,4756(1994)
6. A.Nagashima, N.Tejima and C.Oshima, Phys.Rev.B 50,17487(1994)
7. T.Anazawa, S.Tokumitsu, R.Sekine, E.Miyazaki, K.Edamoto, H.Kato and S.Otani, Surf.Sci.328,269(1995)
8. T.Chiang, G.Kaindl and D.E.Eastman, Solid State Commun. 36,25(1980)
9. K.Christmann and J.E.Demuth, Surf.Sci. 120,291(1982)

10. K.Jacobi, Surf.Sci. 192,499(1987)
11. K.Wandelt, J.Hulse and J.Küpers, Surf.Sci. 104,212(1981)
12. J.Küpers, F.Nitschké, K.Wandelt and G.Ertl, Surf.Sci. 88,1(1979)
13. B.J.Waclawski and J.F.Herbst,Phys.Rev.Lett.35,1594(1975)
14. A.Fujimori, F.Minami and N.Tsuda, Surf.Sci. 121,199(1982)
15. Y.Gamo, A.Nagashima, M.Wakabayashi, M.Terai and C.Oshima,(to be published)
16. T.Kawai, Y.Souzu, M.Tsukada and C.Oshima,(private communication)